Author Version: Marine Geodesy, vol.41(2); 2018; 177-200

Seafloor Geomorphology and Processeson the Western Continental Margin of India based on Multibeam Acoustic Backscatter Data Analysis

SumantaDandapath*[1, 2, 3], Andrew Menezes[1], Bishwajit Chakraborty[1], John Kurian[4], and Koppella N. Prudhvi Raju[3]

[1]CSIR-National Institute of Oceanography, Dona Paula, Goa – 403004, India

[2]Department of Geography,Shivaji University, Kolhapur, Maharashtra – 416004, India

[3]Department of Geography, Banaras Hindu University, Varanasi, Uttar Pradesh – 221005, India

[4]National Centre for Antarctic and Ocean Research, Vasco-da-Gama, Goa – 403804, India

Email: sdandapath@gmail.com (S. Dandapath *Corresponding Author)

bishwajit@nio.org (B. Chakraborty)

Abstract

An assessment of the multibeam sonar data of the central Western Continental Margins of India has been carried out to evaluate the seafloor geomorphology and processes by examining the geomorphological attributes e.g., slope, sediments, structures etc. associated with geomorphic features.The variation in relief and the features located in the region have been mapped and interpreted collectively by utilizing several geospatial mapping tools. The backscatter strength across the area,apparently congruent with the local relief,hashelped to examine the sediment movement on the seafloor.The prominent features found in the region include faults, pockmarks, mounds, submarine terraces and submerged fossil reefs. Several areas with varying topographyengender comparable fractal dimension at shortscale breaks, and the probability density functions (PDFs) utilizing backscatter data depicting overlapping classes.The Present study highlights how fractals and scale break parameters can be utilized to determine the seafloor processes and associated sedimentological dynamics in a complex geographical environment with strong bottom currents, seasonal upwelling, and faulted structure. The role and impact of the various geomorphic processes on the reworking of sediment movement and the overall progression of the seafloor morphology has been revealed for the first time in this part of the ocean bottom.

Keywords: Seafloor geomorphology, Geomorphic processes, Continental margin landforms, Sediment movement, Fractal dimension, Multibeam sonar, Arabian Sea, Mapping

Introduction

Geomorphology as a discipline primarily focuses on the studies of landforms as get reflected by the shape and structure of the earth surface in any geographical location, and the processes responsible for the formation of such landforms (e.g., Hagget 2007). Nowadays, research investigations about geomorphic features and associated processes in the seafloor are also important (e.g., Mayer 2006; Bianco et al. 2014). Most of the research findings and written textbooks in this field exhibit that the seafloor topography is broadly divided into following geomorphologic units having distinct characteristics: continental shelf, continental slope, continental rise, submarine canyon, trench, abyssal plain, and mid-oceanic ridge system (e.g., Trujillo and Thurman 2011; Hu et al. 2015; Mitchell 2015). It is the dynamics of the active seafloor processes, and the geological and environmental importance of a region which attracts researcher for detail investigation. Seafloor characteristics are complex due to variation in many of the parameters at different scales (Fox and Hayes 1985). These parameters involve sediment grain size, relief height at water-seafloor interface and variations within the seafloor sediment volumes. Detail analysis of multibeamechosounding data not only help to understand seafloor morphological complexities but can also be used to identify associated seafloor process (Chen et al. 2016; Lucieer et al. 2016; Palomino et al. 2016). Backscatter data in combination with bathymetry is often used to study reefs, mounds, pockmarks and other small scale seabed features (Garcia et al. 2009; Dandapath et al. 2010; Albarracin et al. 2014; Somoza et al. 2014). Quantitative analysis of multibeam backscatter data also facilitates to characterize seafloor sediment types and hydrocarbon related seepageson the seafloor (Urick, 1983; Goff et al. 2000, 2004; Medialdea et al. 2008; Dandapath et al. 2012).

Semivariogram (semivariance versus lag distance as log-log plot) and spectral techniques address suitably the spatial dependences of the study parameters (Haris et al.2012). For seafloor applications, semivariogram method employing multibeam bathymetry and backscatter data (Herzfeld et al. 1995; Goff et al. 2004) generates distinguishable parameters through the use of statistical techniques such as fractal dimension towards the development of the understanding of the fine-scale aspect of the seafloor. Fractal dimension (characterized by a non-integer exponent unlike surface or a volume) can function as an index reflecting the roughness of the seafloor and other irregularities in the Euclidean space (a metric space that is linear and finite-dimensional) (Barenblatt et al. 1984; Malinverno 1989; Huang and Turcotte 1990; Deems et al. 2006; Chakraborty et al. 2006). In general, the greater the fractal dimensions, the rougher the surface. Such characteristics can be used to distinguish geological provinces of the seafloor. Seafloor topography may possess

multiple features, having varying scales or statistical properties similar to fractional Brownian surfaces, and different fractal dimensions may apply over different scale ranges. Seafloor characteristics of the area are remotely estimated using multi-parameter scattering model (Jackson and Richardson 2007) employing single/multibeamecho-sounding systems operable in high-frequency ranges.

In this paper, an attempt has been made to understand the seafloor geomorphology as contemplated by the slope, sediments, and structures involving detail description and identified geomorphic features, and the associated geomorphic processes on the central Western Continental Margin of India (WCMI) as observed by the multibeam echo-sounding data, sediment data, and other related data. Here estimation of the fine scale seafloor parameters was computed using multibeam bathymetry and backscatter data of high-frequency sonar systems for seafloor characterization and classification (Haris et al. 2011; Chakraborty et al. 2015). Later on elucidating these results within the framework of sediment movements and applied models is explained.

2. Regional setting

The present study area stretches over 105 km² area and lies at 102 km west off Marmagao (offshore Goa) along the central WCMI, in water depths range from 145 m in the northeast to 330 m in the southwest. The general slope is in the direction of west-southwest and increases rapidly towards the deep. The latitudinal and longitudinal extents of the study area is 15°29′50″N to 15°37′30″N and 72°47′13″E to 72°52′27″E respectively. The characteristic of the WCMI, part of which the study area belongs, is regulated by episodic changes and dynamics related to its tectonic evolution, eustatic sea level fluctuations, prevailing geology and sedimentation, the pattern of oceanographic circulation and the biological environment.

2.1. Evolution of the WCMI

The geomorphology of the seafloor along the WCMI is driven by many global and local events occurred in the past. Tectonically the WCMI is part of the Indo-Australian plate; therefore, the origin and evolution of the margin is related to the tectonic and sedimentary processes as evolved before and after the collision of Indo-Australian plate with the Eurasian plate. The WCMI is believed to have formed due to break-up of India from Madagascar during mid-Cretaceous and from Seychelles during the early Tertiary (Courtillot et al. 1988;Bhattacharya and Chaubey 2001). It is believed that a larger area along the western offshore region of India has been submerged in the Arabian Sea; hence, impacting the shape and dynamics of the margin. The crustal structure along the

western continental margin as it appears today is reflecting the pre-existing geology of the region. Eustatic sea level changes over glacial and inter-glacial periods have made their own impacts on the WCMI (Vora 2007) as observed throughout the world (e.g., Cohen et. al. 2016). The evidence still prevails in form of various submerged geomorphic features (e.g., submerged fossil reefs, terraces, buried channels etc.) formed during the respective tectonic, hydrodynamic and sedimentological regimes.

2.2. Geological set-up

The Western Continental Margin of India is a typical passive (Atlantic type) and dissected margin. A number of deep seated faults, fractures, reefs, basement highs, and ridge systems have dissected the area (Bhattacharya and Chaubey 2001; Chakraborty et al. 2006; Mukhopadhyay et al. 2008). The general orientation of these structural features is NNW-SSE and parallel to the coast. The faults in this region are also parallel to the Dharwar Precambrian orogenic trend (Biswas 1987). Recent studies carried out by Chakraborty et al. (2014) deduced that the upper slope region being adjacent to shelf break/edge experiences complex hydrodynamic environment, which also affects sedimentological regime. Bottom Simulating Reflectors (BSRs) and acoustic blanking are detected during recent geological and geophysical surveys (Karisiddaiah and Veerayya 1994; Dewangan and Ramprasad 2007) in the region.

2.3. Oceanographic and biological environment

Regional oceanic circulations characterized by seasonal reversal of monsoon driven surface and bottom currents, summer upwelling and winter downwelling (Naqvi et al. 2010). Bottom currents are strong and wide (~40 km) and run opposite to the direction of surface currents (Shetye et al. 1990). The coast parallel bottom currents move northward (SSE-NNW) carrying low salinity water during southwest monsoon and move southward (NNW-SSE) carrying high salinity water during northeast monsoon. The water depth at which the bottom currents is active ranges between 100 m and 250 m (Rao and Rao 1995). Due to the seasonal upwelling and convective mixing of seawater, the Arabian Sea is one of the most biologically productive regions in terms of faunal abundance and biomass (Ingole et al. 2010). The high biological productivity in combination with slow re-oxygenation producing one of the most intense and thickest Oxygen Minimum Zones (OMZs) observed anywhere in the open ocean (Helly and Levin 2004). This anoxic condition exists in the region for nearly 450 kyr(Ziegler et al. 2010). Most of the studies on benthic community are restricted up to 200 m depth of the margin and are indicates possible influence of environmental factors (Ingole et al. 2010; Haris et al. 2012). Presence of shell materials, high content of calcium

carbonate in sediments and coral structure in the region are evidences of changing dynamics of biological environment over the region.

3. Materials and methods

3.1.Multibeambackscatter image data

The EM1002 multibeam echo-sounding system that was operated for acquiring bathymetric data is installed onboard Coastal Research Vessel (CRV) *SagarSukti* (a research vessel of National Institute of Oceanography, Goa, India), which primarily operates at 95 kHz frequency and possesses 111 pre-formed beams i.e., recording 111 depth values in a single ping. In addition to the depth, the system also records quantitative seafloor-backscatter data, which are utilized to generate backscatter imagery for studying the spatial distribution of the seafloor texture (Tang et al. 2005). In image processing technique, texture provides a measure of coarseness, smoothness or regularity (Cao and Lam 1997). The depth values were recorded in meters (m) and backscatter strength was recorded in decibels (dB) (Blondel 2009). The operating source level of the system is 225 dB re 1μPa at 1 m, and computations of the backscattering strength in dB for each data point was calculated using sonar equations as described in Hammerstad (2005). Real-time gain correction for the EM1002 system is accomplished by applying Lambert's law (which describes exponential decrease of the backscatter strength with respect to incidence angle) i.e., mean backscattering coefficients such as BS_N and BS_O applied at 0º and beyond 25º crossover incidence angles respectively (Simrad model). However, for lower incidence angles (within the 0-25º) the gain settings in the electronics require a reasonably smooth gain change with incidence angle and hence the gain between BS_N and BS_O is linearly changed.Sonar backscatter data corrected in real-time needs improvement to generate images of the seafloor area. This is especially required to remove routine artifacts in the raw backscatter data near the normal beam incidence angles (+/-10º). In addition to the artifacts close to normal incidence beams, the EM1002 backscatter data show residual amplitude due to beam pattern effect, and the real-time system algorithm is unable to compensate such routine situations (Beyer et al. 2007). In order to accomplish the removal of such effect to improve the backscatter data, we have developed a program named as *PROBASI (PROcessingBackscatterSignal) II* (Fernandes and Chakraborty 2009; Haris et al. 2011). The program performs geometric (ship heading, position, bathymetric slope and Lambert's law) corrections. Lambert's law employed throughout the real-time data for gain enhancement of the outer beam signals are required to be removed during the post-processing for compensation. The post-processing procedure was adopted to correct this effect in two stages namely, coarse and fine methods. The coarse method performs the major job of removing center beam and beam pattern

effects. However, the small beam pattern residual persists in the data. Hence, an adaptation of the fine method is necessary for further removal of such residuals. Noise occurring at the transducer tends to get recorded along with the multibeam data, affecting the data quality. To reduce the noise level, the processed output of the fine method is subjected to bandpass filters. Considering the average depth of the seafloor of the study area, a grid size of 10 m x 10 m was utilized to generate backscatter data. The post-processed bathymetry and backscatter data were plotted as xyz point data in ArcGIS and interpolated to rasters(i.e., a matrix of cells having a specific signature). Isobaths of the bathymetry raster were generated and the backscatter range (-51 to -26 dB) was given a color scheme from orange (lowest) to green (highest). Based on the backscatter strength, five segments (see Figure 1) were identified extending over the adjacent area. The range of backscatter strength of segment A', B', C', and D' is equal interval (5 dB) starting from -30 dB to -50 dB.Segment E' is located on a steep slope, in a rather inhomogeneous area compared to other segments, having a wider range of backscatter strength (10 dB) varying from -30 dB to -40 dB. The backscatter responses of the five representative blocks, one each from the segments, arefurther analyzedto understand the prevailing seafloor geomorphology and the processes in the study area.

……..Space for Figure 1……..

3.2. Estimating fractal dimension using semivariogram

Semivariogram method is used to quantify seafloor roughness. The semivariograms were computed utilizing the backscatter data for all the five blocks along with the position data. The type of the semivariogram or the shape of the variogram reveals information about the spatial attributes of the data. For a data point $z(x_n,y_n)$within the block the semivariance $\gamma(h)$, can be estimated as

$$\gamma(h) = \left(1/2n\right)\sum_{n=1}^{n}\left[\left\{z(x_n - y_n)\right\} - \left\{z(x_n - y_n) + h\right\}\right]^2 \text{ ..... (1)}$$

where,*n* is the number of pairs of discrete points separated by a distance *h* (Deems et al. 2006). The semivariograms computed using the above expression show distinguishable signatures for each of the blocks. The processed multibeam data was utilized for computation of 'γ' (Eqn. 1) with a lag distance of 20 m. The fractal dimension is estimated by measuring the slope of the log-log plot of semivariance against the lag distance: *D = 3 – slope/2*.

It has been observed that natural features display fractal properties over a specific range of scales (Mark and Aronson 1984). Normally, least-squares regression analysis of log (semivariance) versus log (lag distance) is used to estimate the fractal dimension ('D'). The 'D' value may vary

continuously with the scale or may involve clear scale breaks with constant fractal dimensions. The scales at which the fractal dimensions change would indicate changes in geomorphic processes and the fractal dimensions could be used to specify the character of the seafloor. To determine the fractal dimension of the identified regions, least squares error fitting between the power law: $\gamma(h) = ah^b$, and semivariogram is obtained to estimate the slope. In this study, the straight line fitting (correlation between data and predicted value) was critically set for a higher correlation coefficient (R^2~0.99). Due to nonlinear nature of the variogram of the backscatter data points, at times proper least square linear error fitting parameters cannot be obtained for higher lag distances and can result in poor correlation i.e., R^2<<0.99, hence segments or windows of such lengths were not chosen for curve fitting. For each data set of the semivariogram, we employed a semi-automated iterative technique to identify the scale breaks in the linear regions of log-log variogram by operating a window function having variable width. To begin with, the window could have maximum width starting from the lowest value of the lag distance (x- axis of the variogram) to its range. The function aims to fit a straight line to this curve by moving the window so that the consecutive points on the curve lie on the straight lines and the R^2 value is determined to ascertain the fitness such that the R^2 is the highest (i.e., R^2~0.99). If all the points cannot lie on the line or in other words R^2<<0.99, the function iteratively adjusts the window length from starting point of the curve from left (the starting point of the variogram) to a point on the curve (towards the range end) by reducing the number of data points till the value of the R^2 is 0.99, and thus first scale break is determined. Similarly, in the subsequent step, the window length starting from previous scale break towards the range end (right) side of the semivariogram is iteratively adjusted using the window function for another straight line fit to determine second scale break having the highest correlation coefficient (R^2~0.99). Though, the correlation values ($R^2 \geq 0.90$) are acceptable (Klinkenberg 1992), however, in the present study, we have computed slope values based on highest possible R^2 values selecting suitable linear segments for multifractal parameter estimations. For example, we have presented two sets of slope values employing linear fits to the semivariogram curve (log-log plot) for block A to estimate the fractal dimensions with varying R^2 values. For block A, R^2 values (0.93 and 0.98) were determined for two 'D' values (2.20 and 2.95) respectively having lag distances of 180 and 320 m respectively. Likewise, by appropriate determination (as mentioned above) of the window length, we obtain different fractal dimensions (2.10 and 2.54) for the total lag distances (120 m) for both the fits within the correlation coefficients (R^2~0.99). Since, the acceptable maximum lag distance for linear curve fitting is 10% of the total distance (1.67 km) i.e., ~160 m (Murata and Saito, 1999), the estimated

data (D) of 2.10 and 2.54 were found appropriate. While estimating 'D' and lag distance values, appropriate curve fitting should be employed so that repeated methods yield the same values.

4. Description of seafloor geomorphology in study area

The description of seafloor geomorphology based on the processed multibeam data in the study area is broadly categorized into slope, sediments, structure and features.

4.1. Slope

The average general slope of the study area is 0.90˚, whereas the slope towards the shallower depth is 0.61˚, and towards the deep this slope changes over to 1.68˚. Based on the measured slope, the study area can broadly be divided into two subdivisions viz., a) gently sloping northeastern part within the 150-220 m water depth, and b) the adjoining steep slope between the 220-330 m water depths in the southwestern part. The local slope in and around some identified geomorphic features (i.e., fault, pockmarks) vary considerably (up to 5˚). Figure 2 shows a variation of local slope in the study area indicating variation in thebathymetry. On the basis of variations of the localslope, the area can be classified into three broad categories: Firstly, smooth terrain or unidirectional sloppy surface having local slope 0-2˚. More than 60% (20% in deep and 90% in the shallow region) of the study area falls under this category. Secondly, moderate terrain, where slope ranges between 2˚ and 3˚, and 35% of the study area (mostly in the deep region) falls under this category. And thirdly rough terrain or undulating surface having local slope more than 3˚. It covers around 3-5% of the study area particularly close to faults, pockmarks and reef structure.

……..Space for Figure 2……..

4.2. Sediments

The present study area is part of a broader continental margin located along the west coast of India having identical oceanographic conditions. Therefore, recent sedimentological studies in surrounding areas may be comparable to the present investigation. Sediment cover in the region is up to 4 km thick with a higher proportion of total organic carbon (2-4%) having a marine origin (Naqvi et al. 2010; Calvert et al. 1995). The inner section of the continental shelf is represented by recent clayey sediments while the outer shelf is covered by relict sands (Rao and Wagle 1997). The surficial sediments of the upper continental slope are clayey sand (50% sand, 31% clay,and 19% silt) (Rao and Veerayya 2000) and the lower and mid-slope is covered by silty clay with an admixture of dominant terrigenous and biogenic components (Rao and Rao 1995). Sedimentological studies indicate that the outer shelf represents a paleo-beach environment (Shankar and Karbassi 1992).

Calcium carbonate ($CaCO_3$) and sand content in the surface sediments (Thamban et al. 1997) is also higher (61% and 33% respectively within the 2-4 cm core depth).

In the present study area, deep sediment cover, a higher proportion of hydrogen-rich (marine origin) organic carbon (Paropkari et al. 1993), and its good preservation by a permanent oxygen-minimum zone create ideal conditions for the generation of hydrocarbon in the subsurface sediments. Seasonal upwelling, strong bottom currents (Shetye et al. 1990) and moderate to steep gradient, leading to a cross-shelf transport of clay minerals towards the mid-slope or lower slope region (Figure 3) (Rao and Wagle 1997). The sediment sample data acquired using Van Veen grab (SagarSukti cruise no. 168) show association of abundant shell components. In this area, clayey sand and sandy sediment types are observed to be associated with the moderate to abundant shell materials. Moreover, in some locations sandy sediment without shell materials are also seen. Generally, higher acoustic backscatter strengths (-35 dB) in the deeper water (at or near pockmark zone) suggest coarse-grained sediment at the seafloor due to increased acoustic impedance (Wen and Larsen 1996; Endler et al. 2015) and roughness related scattering (Goff et al. 2000), which is linked to the precipitation of diagenetic minerals from the biodegradation of seepage material (Loncke and Mascle 2004; Logan et al. 2010).Such backscatter variability is also functional to the seafloor slope, sediment type and relief (Blondel and Murton 1997). In shallow water (<210 m) where seabed gradients are gentle, normally backscatter strength is low beside few occasional discrete curvilinear, circular or clustered patches of higher backscatter (-32 dB). This area is possibly covered by a thin layer of soft terrigenous clayey mud producing average seafloor backscatter strength (-45 dB). The variation in backscatter observed between these different areas is broadly comparable with results of calibrated acoustical measurements between different known sediment types (e.g., Urick 1983).

……..*Space for Figure 3*……..

4.3. Structures and features

The self-slope margin with incremental steep slope towards the deep and number of faults, fractures, reefs, basement highs and ridge system in the surrounding regions are identified (Chakraborty et al. 2006; Mukhopadhyay et al. 2008). The study area exhibit the presence of a number of NNW-SSE trending faults dissecting the area (Figure 3). A stretch of single-beam echo-sounderprofile (frequency: 33 kHz) across the centre of the study area (15º33′N latitude) reveals two faults. Pockmarks are the main geomorphic features in the region. The origin and evolution of pockmarks and related seepages have greatly influenced the shaping of the seafloor in the study area. Besides, the fault system in the region has also played a major role in themorphological evolution of

the surrounding seafloor. Submarine terrace,reef structure, and small mounds are the other notable geomorphic features observed in the study area (Figures 3 and 4). However, the complete morphology of the seafloor in the study area is possibly driven by the combined influence of various processes i.e., seafloor seepages, faulting and related tectonic activities, and sediment movements by bottom currents, gravity flow (across slope) and submarine slumping.

……..Space for Figure 4……..

4.3.1 Pockmarks

Pockmarks are hemispherical depressions often observed in the seep venting areas of the seafloor (Hovland and Judd 1988). Pockmarks are normally considered as the surface expressions of the presence of shallow gas or deep-seated gas hydrates. Due to the emission of greenhouse gasses (mostly methane) through them the study of pockmarks are important. In the present study area, total 112 pockmarks were identified most of which are associated with the NNW-SSE trending faults (Figure 3). The shape and orientation of these pockmarks are influenced by the direction of bottom currents (Dandapath et al. 2010). Interestingly, these pockmarks are observed nearly 50 km away from a BSR zone. Description of pockmarks with every possible detail along with the comparison with their global counterparts was reported by Dandapath et al. (2010). Presence of possible buried pockmarks is also reported from the region.

……..Space for Figure 5……..

4.3.2 Faults and fractures

The lineaments like faults and fractures have often bridged the links between earth surface and the deep crust and create weakness in the region. Such weaknesses sometimes trigger a larger movement of tectonic forces which otherwise seemed to be inactive for a long time. The existing fault system has a greater role in the regional geomorphology in the central WCMI. Multibeam bathymetry (Figure 3), a single-beam echosounder profile (Figure 4) and single channel sparker section along with corresponding sub-bottom profiler (Figure 5) has helped to locate three distinct faults and their close association with the pockmarks in the study area including seepage locations. These shallow faults are possibly linked to either i) Bottom Simulating Reflector (BSR) zone in the slope region (Dewangan and Ramprasad 2007) or ii) the subsurface reservoir of hydrocarbon bearing sediments in the deep, and thus might have carried the fluid to the surface leading to the formation of pockmarks in the region. Among the three identified faults in the area, the impact of the centrally located fault is much higher on the morphology of the surrounding seafloor. The central fault also

witnessed a maximum number of pockmarks along its axis. The observed backscatter strength is stronger (-30 to -38 dB) in and around the faults. Gradual changes in bathymetry along a line within the middle of the study area parallel to the fault also seen. This is somehow similar to a fracture, possibly formed in past and covered by the sediments.

4.3.3 Terraces

The presence of submarine terraces at various depths along the western continental margin of India was reported by Wagle et al. (1994). These terraces are assumed to have been formed during glacial ages when the coastline was at much lower depth than the present (Martinez-Martos et al. 2016; Reis et al. 2013). The identified submarine terrace (located at around 205 m depth in the study area) as observed in multibeam bathymetry map and single beam echosounder (33 kHz) profile is marked in Figures 3 and 4 respectively. In the present study identified terraceis not extensive possibly due to the result of self-edge subsidence after its formation (Vora 2007). The relief difference is also minimal. The higher sediment movement by active bottom currents in the region may also have influenced their present day shape and structure.

4.3.4 Reefs

Submerged reefs are defined as reefs that were established in relation to the pre-existing sea levels (Linklater et al. 2015). In the north-east corner of the study area between 150 m and 170 m depth a fragmented reef structure having a number of peaks is observed (Figure 3). The sediment samples collected from the nearby regions show higher proportions of calcium carbonate along with the presence of shell materials. The backscatter strength is also significantly higher than the nearby region.

The presence of fossil reef at 160 - 170 m depth and terrace-like structure at 205 m depth indicate that the maximum relative sea level drop in the region was perhaps more than it believed (Reis et al. 2013). It may be possible that the submerged Konkan coast, higher rate of subsidence along self-edge (Vora 2007) and very thick layer of sediments in the region (Calvert et al. 1995) either in isolation or in combination are hiding many geomorphic features that have originated during that time on the outer shelf of the central WCMI. The anomalous signatures of backscatter without having any indication of the presence of pockmarks may possibly helpful identifying them.

4.3.5 Mounds

Mounds are known to be developed in regions where shallow gasses are present. They are positive relief expressions opposite to pockmarks but may occur in association with the pockmarks

(Hovland and Judd 1988). In the present study area, mounds are small (0.5 – 1.5 m vertical relief) and located on the eastern side next to relatively large sized pockmarks (Figure 3). Most of them are placed very near to the central fault. Association of these mounds with the pockmark suggests that gas/fluid is perhaps initially migrated towards the mound. These mounds are possibly formed by the gasses that are stored in the pore spaces of the sub-surface sediments especially in the upslope side of pockmarks (due to gravitational pull-up) even after the initial gas expulsion took place (through the downslope side) leading to the formation of pockmarks. The left out gasses could not be released through the pockmarks, or build up enough pressure to form another outbreak due to cut off of gas supply. Gas stored upslope side and beneath the small mounds may be causing high backscatter and apparently helped to map the seepages in the study area (Dandapath et al. 2012).

5. Understanding seafloor geomorphic processes in the central WCMI

Quantitative analysis (fractal dimension estimation based on semivariogram method, and curve fitting) of multibeam echo-sounder data primarily the backscatter data, was made to detect the prevailing geomorphic processes over the study area. Seafloor roughness was studied in the past using fractal dimension parameter of the depth (Fox and Hayes 1985; Malinverno 1989),and backscatter images (Dandapath et al. 2012).The fractal dimension is used to measure the degree of fragmentation and irregularities linked to the behavior of the system (Mandelbrot 1977, 1983). Monofractals are homogeneous objects having same scaling properties, and characterized by a single singularity exponent (Stanley et al. 1999).Many of the fractals observed in nature have infinite hierarchy of statistical exponents that offer a convenient framework to quantify the complex systems. Therefore, processes cannot be said monofractal for more complicated cases where different scaling exponents can be revealed for many interwoven fractal subsets of time series, and such processes are recognized as multifractals (Telesca et al. 2002; Chakraborty et al. 2014; Haris and Chakraborty 2014). The multibeam backscatter data often show volumetric characteristics of the seafloor (Jackson and Richardson 2007), which can be useful to understand the processes if carefully analyzed. Therefore, backscatter data is more vigorously used for this purpose. The segmented area and their representative blocks are shown in Figure 1.

5.1. Observation of the backscatter probability density function (PDF) data

The statistical details of the five blocks (A-E) with backscatter data points (1,411 to 1,512) associated with each of the segmented area (A'-E') is given in Table 1. The PDFs of these blocks (backscatter data) are shown in the Figure 6. The highest average backscatter value (-32.3 dB) lies in block A within the range (-35.8 to -26.3 dB). Similarly, blocks B, C, D and E, have mean backscatter

values as -37.4 dB, -43.1 dB, -48.5 dB and -36.9 dB respectively. The ranges vary between (-32.4 to -41.6 dB), (-41.4 to -45.1 dB), (-51.4 to -43.4 dB), and (-29.4 to -42.1 dB) for the blocks B, C, D and E respectively. Figure 6 depicts bar graphs indicating an almost distinct segmentation for the backscatter strength data except for the overlapping PDFs of the block areas B and E. The location of the blocks (Figure 1), in conjunction with the overlapping PDFs suggests gravity induced sediment movement due to the steep slope along the fault zone.

……..Space for Table 1……..

……..Space for Figure 6……..

5.2. Observation of the bathymetry and backscatter profiles

In order to understand the complexity of the seafloor morphology backscatter strength of five blocks are shown in enlarged view (Figure 7a). Backscatter and depth profiles taken along the central line of the five blocks is depicted in Figures 7b and c. Block A situated close to fault zone has undulating depth and backscatter profiles (with highest backscatter strength) throughout the section. The block is crossed by a fault plane and encompasses comparatively a steep slope. Two pockmarks having depths 2.4 m and 1.3 m with diameters 120 m and 125 m, respectively, and elongated in shape are observed in block A (Figure 7a). Block B stretches between the two fault zones 1.3 km apart without any pockmarks, with backscatter strength profile (Figure 7c) that is less fluctuating and smooth seafloor topography (Figure 7b).

……..Space for Figure 7……..

The topographic profile of the block C is smooth and the backscatter shows gentle variations with decreased strength. The clayey sand deposition on the inner slope, as observed in the acquired sediment data, is indicative of slow mass movement of sediments (Rao and Rao 1995). The bathymetric profile of block D is indicative of smooth topography, however the backscatter profile indicates comparable undulations with respect to the backscatter profile of block A. Block E with three moderate sized pockmarks (maximum pockmark depth: 5.0 m and diameter: 140 m) shows variations in topographic and backscatter profiles. This block is situated in the relatively deeper part of the study area. In general, the undulation in the backscatter strength of block E is similar to that of block B located at the middle of the study area.

5.3. Understanding processes using fractal dimension (D)

Log-log plots of the semivariogram of the backscatter data of the five blocks are presented in Figure 8. Estimated ‘D’ values for five data blocks are given in Table 2. The semivariogram plot for

block A shows strong power law distributions over two segments, separated by a relatively distinct scale break. The short range window is characterized by lower 'D' (2.10), whereas 'D' is higher (2.54) for the longer range. Interestingly for block D, the estimated fractal dimensions are similar to A (Table 2). The mean backscatter strength (-32.3 dB) is the highest for the block A (within the steep fault zone) whereas block D possesses the lowest mean backscatter strength (-48.5 dB).

……..*Space for Figure 8*……..

……..*Space for Table 2*……..

As stated earlier, the seafloor topographic profile of block A is comparatively undulating (Figures 7b and c) than the block D. Though the short and long range 'D' values of block D are similar to that of block A, the area under block D possesses a different sediment texture, i.e., the block A seafloor area has coarser sediment texture than that of the top sedimentary layer (clayey sand) of block D (CRV SagarSukti expedition report no. 168). There is no relationship between the backscatter level and topographic data of block D (Figures 7b and c). Though the fractal dimension values are comparable indicating backscatter pattern changes are similar for both the areas, the scale break distances are not the same. The long range scale break of block D, vary within the limits of 120-380 m range compared to the 140-200 m range for block A. The accumulation of clay sediment due to the cross-shelf transport has been reported earlier (Rao and Rao 1995), i.e., the turbidites transported across the shelf area have been reported in the eastern Arabian Sea basin. However, due to the location of block A near a relatively steep slope, the upper slope is devoid of fine sediment. Though the locations of these two blocks (A and D) and their parameters of the log-log plots of the semivariogram versus lag distances and corresponding backscatter strengths are noticeably different, however, the similarity in 'D' values of the two different environments is noteworthy. Due to the existence of fine sediment layer overlying coarse sediments of block D as compared to block A, the backscatter levels of block D are found to be lower, which may be related to the signal attenuation (due to the clayey sediment on the top). The short range scale break of block D (indicating small scale seafloor roughness as 'D' value is small) is relatively shorter (60-100 m) than that of the block A (60-120 m) (Table 2). The existence of smooth topographic profile and undulating backscatter data suggest the influence of considerable sediment movement in the D block area. The comparable fractal dimensions and the variation in scale break parameters from two different sections of the seafloor (i.e., block A and D), exhibit the importance of studying the scale break parameters (Sun et al. 2006). Conceptually higher scale break distance of longer ranges of block D indicate that the

boundaries between the homogenous regions are larger than the block A backscatter data even for similar ‘D’ values.

It is observed that the fractal dimensions of blocks B and E for the short ranges scale break are the same (2.25) (Figure 8 and Table 2). However, the short range scale break of block E (60-140 m) is larger than that of B (60-100 m). Moreover, the ‘D’ values with respect to the long-range scale breaks of B and E blocks are very high, i.e. 2.71 and 2.82, respectively, with scale breaks within 120-220 m and 160-360 m. Interestingly the backscatter values of blocks B and E have a comparable average (i.e. -37.4 and -37.0 dB respectively). In general, the ranges of the backscatter variations of both the areas are quite similar and the PDF plots of the backscatter data show an overlap indicating similar textures. The topographic fluctuations of block E are comparatively higher than block B (Figure 7b). Block E is located towards the deeper valley side of the fault zone (Figure 3). However, similar backscatter strength, as well as small-scale roughness (short scale break range 'D' values), can be related with the transported sediment from the shallower areas (block B) (Chakraborty et al. 2006).The average backscatter value for block C is -43.1 dB that significantly differs with respect to block D (Table 1), even though they are closely located. Though the topographic profile of block C indicates a smooth seafloor, the backscatter profile exhibit low amplitude sinusoidal variation (Figure 7b). Such variation is difficult to infer from bathymetric data. The ‘D’ values: 2.45 and 2.75 are estimated from the semivariogram plot having scale break starting from 60-100 m and 120-200 m respectively (Figure 8 and Table 2). The comparatively higher value of the ‘D’ towards the short range end of the scale break indicates dominant small scale roughness due to the overlying fine sediment.

5.4. Understanding the seafloor processes using estimated multi-modal parameters

The present study highlights the existence of more than one ‘D’ value for all the blocks, which suggests the involvement of more than one seafloor process acting in the study area. Such physical processes may be responsible for multi-modal seafloor. The active physical processes influence seafloor sediment movement i.e., reworking on the seafloor that ultimately results in changes in seafloor roughness. These phenomena are reflected in the remotely acquired multibeam backscatter data of the present study. In this part of the western continental margin, the underwater bottom currents are active in water depth interval between the 100-250 m and within a width of 40 km (Rao and Rao 1995). The dominant bottom currents during southwest monsoon (June-September) and north-east monsoon (November-February) are reported by Shetye et al. (1990). The directions of currents are shown in Figure 1. Mela and Louie (2001) had made a comparison between

the estimated ‘D’ values employing ‘slope’ of the semivariogram and Fourier techniques. Their application for high-resolution seismic sections shows well matched ‘D’ values. In this work, similar comparisons have been examined to support the observations made in this study for multimodal seafloor inferred through semivariogram study. The estimated slope and corresponding ‘D’ values using power spectral density function of the multibeam backscatter data (middle line of the five study blocks) match well with the ‘D’ values estimated using semivariogram method. Employing micro-bathymetric data, Stewart et al. (1994)also used power spectral density function to establish the existence of multimodal for three types of ridge seafloor areas which provided more than one slope parameter. In order to further confirm the seafloor multimodal parameters, curve fitting of the PDF curves of the backscatter data were carried out.

Fitting distributions consist of finding a mathematical function which represents a suitable statistical variable. There are three steps in curve fitting of the PDF: i) model/function choice, ii) estimate parameters, and iii) evaluate the quality of fit i.e., the goodness of fit tests. Accordingly, we have chosen individual distribution as a Gaussian function (Gonidec et al. 2003)to represent the data mathematically by a mixture of more than one model (i.e., the Gaussian mixtures model)to estimate the required model parameters for further analysis. Amongst the different estimation methods, we have employed Maximum Likelihood Estimation (MLE), which is used in statistical inference to estimate parameters. MLE begins with the mathematical expression known as a likelihood function of the sample data. Generally, the likelihood of a set of data is the probability of obtaining that particular set of data given the chosen probability model. For MLE, the expression contains unknown parameters, and these parameters maximize the sample likelihood. Estimated proportions, means and standard deviation without constraints (i.e., floating) are provided after a few iterations, and a good fit of overall and component populations are obtained along with their mean and standard deviations (Table 3). In the present study, a number of iterations employed for MLEs are lying within 314-331 for the five blocks. In order to check the quality of the test, Kolmogorov-Smirnov goodness of fit is used. The statistical significance of the overall fit using corresponding PDFs is employed. The fitted parameters are acceptable since they are within the 98-99% for the five blocks. Observations of the fitted curves indicate reasonably good fit except data of block D. Presented PDFs and fitted curves are normalized with respect to the highest value of the block E (Figure 9). In general, the figure indicates well fitted multi-modal curves for all the five blocks. The existence of more than one population corroborates well with the multifractal results observed in semivariogram studies (Table 3).

……..Space for Table 3……..

……..Space for Figure 9……..

5.5. Summary of observation on active geomorphic processes

Based on the present observations and recent reporting (e.g., Dandapath et. al.2010, 2012; Chakraborty et. al. 2015) from the region, it can be surmised that the overall geomorphology in the central WCMI is an outcome of the combined effect of (i) higher rate of sedimentation, (ii) seafloor hydrocarbon seepages, (iii) tectonic related faulting, (iv) seasonal bottom currents, and (v) gravity induced cross-slope mass movement. The high rate of sedimentation is probably burying the normal surface expression of geomorphic features which is evident from the presence of buried pockmarks as well as the unexpected variation of relief of identified features in the region. Seafloor hydrocarbon seepages triggered/stimulated by tectonic related faulting across the region is responsible for the formation of numerous number of pockmarks and small mounds. Likewise, seasonal (monsoon related) bottom currents is responsible for along coast sediment displacement particularly in the shallower part which affect the morphology of features, whereas, gravity induced cross-slope mass movement promotes the movement of soft sediments in particular. These active geomorphic processes in combination along with small scale tectonics and sea level change have been probably shaping the evolution of the landscape geomorphology of the seafloor in the central WCMI.

6. Conclusions

The present study demonstrates the fine scale changes of seabed slopes at varying water depth and their impact on sediment transport pattern along the shelf-slope margin of the central WCMI. The pattern of local slope suggests variable roughness across the study area and a clear distinction of seafloor relief in and around the faults, pockmarks and other associated features in the region. The sediments are mainly clayey sand type with dominating shell materials with an admixture of high organic carbon content. The sediment movement in the shallow region is primarily due to active bottom currents. In the deeper region, relatively higher seafloor slope plays an important role. Most of the prominent features (if not all) are oriented in the direction of NNW-SSE, parallel to the coast and opposite of the seafloor gradient.

The geomorphic features that have been found in the study area are pockmarks, faults, mounds, terrace and fossil reefs. The pockmarks are more widespread than any other features and have greatly contributed to the seafloor morphology of the study area. Out of the three faults observed in the region, the centrally located fault at around 230 m water depth has influenced the

most. Mounds are occasionally associated with pockmarks and faults towards the headwall side. The terrace and the reef structure are located in relatively shallow region and are fragmented in nature. The pockmarks and mounds are believed to have originated due to seafloor seepages of gas/fluid, whereas the reef structure and terrace seen here are the outcome of eustatic sea level changes and/or large scale submergence of the region. The higher sediment movement by active bottom currents in the region may also have influenced present day shape and structure of these features.

For the first time multiscale analyses were carried out to understand seafloor processes involving backscatter data and the estimation of fractal dimensions. The present research underscores the importance of backscatter data alongside with the bathymetry for analysis and interpretation of overall seafloor geomorphology. The use of backscatter data is particularly important to evaluate the active seafloor processes and the sediment movement in an ever-changing environment. The backscatter strength appeared to have progressively altered as the seafloor gradient slowly changed with the increasing depth, and is sharply interrupted along the deep valley region close to fault zone. A general comparison of the seafloor topography and backscatter data indicates that the backscatter intensities are higher and show more fluctuations (rough) towards the outer slope areas. Whereas in the shallow areas where topographic roughness is less, the corresponding backscatter strength appeared to have reduced due to clayey sand sediments. There is some resemblance in variation of backscatter strength at different water depth in study area, possibly related to the fine sediment movement due to turbidity in the shelf-slope region. The relationship between the backscatter Probability Density Functions (PDFs) and the corresponding fractal dimension values at different scale breaks within the study area signify comparable sedimentary processes with varying degrees, which could be due to gravity induced sediment movement following the general slope of the study area.

Acknowledgements

The authors are thankful to the Director, CSIR-National Institute of Oceanography, for his permission to publish this work. The critical review by the editor and the reviewers is appreciable and has substantially improved the quality of the manuscript. The multibeam data was acquired under the Exclusive Economic Zone mapping program of the Ministry of Earth Sciences, Govt. of India. This paper is partly based on the thesis submitted for PhD by SD at Banaras Hindu University, Varanasi, India. This is NIO contribution number xxxx.

References

Albarracin S., J. Alcantara-Carrio, I. Montoya-Montes, A. Fontan-Bouzas, L. Somoza, C. L. Amos, and J. R. Salgado. 2014. Relict sand waves in the continental shelf of the Gulf of Valencia (Western Mediterranean). *Journal of Sea Research* 93:33-46.

Barenblatt, G. I., A. V. Zhivago,Y. P. Neprochnov, and A. A. Ostrovskiy.1984. The fractal dimension: a quantitative characteristic of ocean-bottom relief. *Oceanology* 24:695-697.

Beyer, A., B. Chakraborty, and H. W. Schenke. 2007. Seafloor classification of the mound channel provinces of the Porcupine Seabight: an application of the multibeam angular backscatter data. *International Journal of Earth Sciences (GeolRundsch)* 96:11-20.

Bhattacharya, G. C. and A. K. Chaubey. 2001. Western Indian Ocean – A Glimpse of the Tectonic Scenario, InTheTndian Ocean – A Perspective. Gupta R. S. and E. Desa (eds.), New Delhi: Oxford-IBH, 691-729.

Bianco, F. D., L. Gasperini, F. Giglio,G. Bortoluzzi, Z. Kljajic, and M. Ravaioli. 2014. Seafloor morphology of the Montenegro/N. Albania Continental Margin (Adriatic Sea-Centra Mediterranean). *Geomorphology* 226:202-216.

Biswas, S. K. 1987. Regional tectonic framework, structure and evolution of the western marginal basins of India. Tectonophysics 135:307-327.

Blondel, P. 2009.*The Handbook of Sidescan Sonar*.Chichester, UK: Springer and Praxis Publishing.

Blondel, P. and B. J. Murton. 1997.*Handbook of Seafloor Sonar Imagery*. Wiley-praxis series in Remote Sensing.Chichester: John Wiley and Sons Ltd.

Calvert, S. E., T. F. Pedersen, P. D. Naidu, and U. von Stackelberg. 1995.On the organic carbon maximum on the continental slope of the eastern Arabian Sea. *Journal of Marine Research* 53:269-296.

Cao, C. and N. S. Lam. 1997.Understanding the scale and resolution effects in remote sensing and GIS.In*Scale in remote sensing and GIS*.Quattrochi, D. A. andM. F. Goodchild (eds.),Boca Raton: CRC press, 57-72.

Chakraborty, B., R. Mukhopadhyay, P. Jauhari, V. Mahale, K. Shashikumar, and M. Rajesh.2006. Fine-scale analysis of shelf-slope physiography across the western continental margin of India. *Geo-Marine Letters* 26:114-119.

Chakraborty, B., K. Haris, G.Latha, N. Maslov, and A. A. A. Menezes. 2014. Multifractal approach for seafloor characterization. *IEEE Geoscience and Remote Sensing Letters* 11:54-58.

Chakraborty, B., A. A. A. Menezes, S. Dandapath, W. A. Fernandes, S. M. Karisiddaiah, K. Haris, andG. S. Gokul. 2015. Application of hybrid techniques (self-organizing map and fuzzy algorithm) using backscatter data for segmentation and fine-scale roughness characterization of the seepage-related seafloor along the western continental margin of India. *IEEE Journal of Oceanic Engineering* 40:3-14.

Chen, H., W. Zhan,and S. Wu. 2016. Response of geomorphic and geological processes to insufficient and ample sediment supply along the upper continental slope in the north-western South China Sea. *Journal of Earth System Science* 125: 1635-1655.

Cohen, M. C. L., R. J. Lara, E. Cuevas, E. M. Oliveras, and L. D. S. Sternberg. 2016. Effects of sea-level rise and climate changes on mangroves from southwestern littoral of Puerto Rico during the middle and late Holocene. *Catena* 143:187-200.

Courtillot, V., G. Feraud, H. Maluski, D. Vandamme, M. G. Moreau, and J. Besse. 1988. Deccan flood basalts and the Cretaceous/Tertiary boundary. Nature 333:843-846.

Dandapath, S., B. Chakraborty, S. M. Karisiddaiah, A. Menezes, G. Ranade, W. Fernandes, D. K. Naik, andK. N. PrudhviRaju. 2010. Morphology of pockmarks along the western continental margin of India: Employing multibeam bathymetry and backscatter data. *Marine and Petroleum Geology* 27:2107-2117.

Dandapath, S., B. Chakraborty,N. Maslov,S. M.Karisiddaiah, D. Ghosh, W. Fernandes, and A. Menezes. 2012. Characterization of sea floor pockmark seepage of hydrocarbons employing fractal: A case study from the western continental margin of India. *Marine and Petroleum Geology* 29:115-128.

Deems, J. S., S. R. Fassnacht, and K. J. Elder. 2006. Fractal distribution of snow depth from LiDAR data. *Journal of Hydrometeorology*7:285-297.

Dewangan, P. and T. Ramprasad. 2007. Velocity and AVO analysis for the investigation of gas hydrate along a profile in the western continental margin of India. *Marine Geophysical Research* 28:201-211.

Endler, M., R. Endler, B. Boboretz, T. Leipe, and H. W. Arz. 2015. Linkage between acoustic parameters and seabed sediment properties in the south-western Baltic Sea. *Geo-Marine Letters* 35:145-160.

Fernandes, W. and B. Chakraborty.2009.Multi-beam backscatter image data processing techniques employed to EM 1002 system. *Proceedings of the International Symposium on Ocean Electronics (SYMPOL 2009)*.Department of Electronics, Cochin University of Science and Technology, Kochi, India.

Fox, C. G. andD. E. Hayes. 1985. Quantitative methods for analyzing the roughness of the seafloor. *Reviews of Geophysics* 23:1-48.

Garcia, M., F. J. Hernandez-Molina, E. Llave, D. A. V. Stow, R. Leon, M. C. Fernandez-Puga, V. D. Rio, and L. Somoza. 2009. Contourite erosive features caused by the Mediterranean outflow water in the Gulf of Cadiz: Quaternary tectonic and oceanographic implications. *Marine Geology* 257:24-44.

Goff, J. A., H. C. Olson, and C. S. Duncan.2000. Correlation of side-scan backscatter intensity with grain-size distribution of shelf sediments, New Jersey margin. *Geo-Marine Letters* 20:43-49.

Goff, J. A., B. J. Kraf,L. A. Mayer, S. G. Schock, C. K. Sommerfield, H. C. Olson, S. P. S. Gulick, and S. Nordfjord.2004. Seabed characterization on the New Jersey middle and outer shelf:

correlatability and spatial variability of seafloor sediment properties. *Marine Geology* 209:147-172.

Gonidec, Y. L., G. Lamarche, andI. C. Wright. 2003. Inhomogeneous substrate analysis using EM300 backscatter imagery. *Marine Geophysical Research* 24:311-327.

Hagget, R. J. 2007.*Fundamentals of Geomorphology*.London: Routledge.

Hammerstad, E. 2005.*EM technical note: Sound level from Kongsberg multibeam*. Kongsberg Simrad, Norway.

Haris, K., B. Chakraborty, C. De, R. G. Prabhudesai, and W. A. Fernandes. 2011. Model-based seafloor characterization employing multi-beam angular backscatter data - A comparative study with dual-frequency single beam. *Journal of the Acoustical Society of America* 130:3623-3632.

Haris, K., B. Chakraborty, B. S. Ingole, A. A. A. Menezes, andR. Srivastava. 2012.Seabed habitat mapping employing single and multi-beam backscatter data: A case study from the western continental shelf of India. *Continental Shelf Research* 48:40-49.

Haris, K. andB. Chakraborty.2014. Stochastic formalism-based seafloor features discrimination using multifractality of time-dependent acoustic backscatter. *Nonlinear Processes in Geophysics* 21:101-113.

Helly, J. J. and L. A. Levin. 2004. Global distribution of naturally occurring marine hypoxia on continental margins, Deep-Sea Research II 51:1159-1168.

Herzfeld, U. C., I. I. Kim, and J. A. Orcutt. 1995. Is the ocean floor a fractal? *Mathematical Geology* 27:421-462.

Hovland, M. andA. G. Judd. 1988.*Seabed Pockmarks and Seepages Impact on Geology, Biology and the Marine Environment*. London, UK: Graham & Trotman.

Hu, M. Z., J. C. Li, H. Li, C. Y. Shen, T. Y. Jin, and L. L. Xing. 2015. Predicting Global Seafloor Topography Using Multi-Source Data. *Marine Geodesy* 38:176-189.

Huang, J. andD. L. Turcotte.1990.Fractal image analysis: application to the topography of Oregon and synthetic images. *Journal of the Optical Society of AmericaA* 7:1124-1130.

Ingole, B. S., S. Sautya, S. Sivadas, R. Singh, and M. Nanajkar. 2010. Macrofaunal community structure in the Western Indian Continental Margin including oxygen minimum zone. Marine Ecology 31:148-166.

Jackson, D. R. and M. D. Richardson.2007.*High-Frequency Seafloor Acoustics*. New York: Springer.

Karisiddaiah, S. M. and M. Veerayya. 2002. Occurrence of pockmarks and gas seepages along the central western continental margin of India. Current Science 82:52-57.

Klinkenberg, B. 1992.*Fractals and morphometric measures: is there any relationship?* Geomorphology 5:5-20.

Linklater, M., B. P. Brooke, S. M. Hamylton, S. L. Nichol, and C. D. Woodroffe. 2015. Submerged fossil reefs discovered beyond the limit of modern reef growth in the Pacific Ocean. *Geomorphology* 246:579-588.

Logan, G. A., A. T. Jones, J. M. Kennard, G. J. Ryan, and N.Rollet.2010. Australian offshore natural hydrocarbon seepage studies, a review, and re-evaluation. *Marine and Petroleum Geology* 27:26-45.

Loncke, L. and J. Mascle. 2004. Mud volcanoes, gas chimneys, pockmarks and mounds in the Nile deep-sea fan (Eastern Mediterranean): geophysical evidence, *Marine and Petroleum Geology* 21:669-689.

Lucieer, V., Z. Huang, and J. Siwabessy. 2016. Analyzing Uncertainty in Multibeam Bathymetric Data and the Impact on Derived Seafloor Attributes. *Marine Geodesy* 39:32-52.

Malinverno, A. 1989.Testing linear models of sea-floor topography.*Pure and Applied Geophysics* 131, 139-155.

Mandelbrot, B. B. 1977.*Fractals: Form, Chance, and Dimension*. San Francisco: Freeman.

Mandelbrot, B. B. 1983.*The Fractal Geometry of Nature*.New York: Freeman.

Mark, D. M. And P. B. Aronson. 1984.Scale-dependent fractal dimensions of topographic surfaces: An empirical investigation, with applications in geomorphology and computer mapping. *Mathematical Geology*16:671-683.

Martinez-Martos, M., J. Galindo-Zaldivar, F. J. Lobo, A. Pedrera, P. Ruano, M. Lopez-Chicano, and M. Ortega-Sanchez. 2016. Buried marine-cut terraces and submerged marine-built terraces: The Carchuna-Calahonda coastal area (southeast Iberian Peninsula). *Geomorphology* 264:29-40.

Mayer, L. A. 2006.Frontiers in seafloor mapping and visualization.*Marine Geophysical Research* 27:7-17.

Medialdea, T., L. Somoza, R. Leon, M. Farran, G. Ercilla, A. Maestro, D. Casas, E. Llave, F. J. Hernandez-Molina, M. C. Fernandez-Puga, and B. Alonso. 2008. Multibeam backscatter as a tool for sea-floor characterization and identification of oil spills in the Galicia Bank. *Marine Geology* 249:93-107.

Mela, K. and J. N. Louie. 2001.Correlation length and fractal dimension interpretation from seismic data using variograms and power spectra. *Geophysics* 66:1372-1378.

Mitchell, N. C. 2015.Submarine Geomorphology (Chapter 09249).In *Reference Module in Earth Systems and Environmental Sciences*.Elsevier. DOI: http://dx.doi.org/10.1016/B978-0-12-409548-9.09249-6.

Mukhopadhyay, R., M. Rajesh, S. De, B. Chakraborty, andP. Jauhari. 2008. Structural highs on the western continental slope of India: Implications for regional tectonics. *Geomorphology* 96:48-61.

Murata, S. andT. Saito. 1999. The variogram method for a fractal model of rock joint surface. *Geotechnical and Geological Engineering* 17:197-210.

Naqvi, S. W. A., H. W. Bange,L. Farias, P. M. S. Monteiro, M. I. Scranton, andJ. Zhang. 2010. Marine hypoxia/anoxia as a source of CH_4 and N_2O. *Biogeosciences* 7:2159-2190.

Palomino, D., J. Vazquez, L. Somoza, R. Leon, N. Lopez-Gonzalez, T. Medialdea, L. Fernandes-Salas, F. Gonzalez, and J. A. Rengel. 2016. Geomorphological features in the southern Canary Island Volcanic Province: The importance of volcanic processes and massive slope instabilities associated with seamounts. *Geomorphology* 255:125-139.

Paropkari, A. L., C. P. Babu, andA. Mascarenhas. 1993. New evidence for enhanced preservation of organic carbon in contact with oxygen minimum zone on the western continental slope of India. *Marine Geology* 111:7-13.

Rao, V. P. and B. R. Rao. 1995. Provenance and distribution of clay minerals in the sediments of the western continental shelf and slope of India. *Continental Shelf Research* 15:1757-1771.

Rao, V. P. andB. G. Wagle. 1997. Geomorphology and surficial geology of the western continental shelf and slope of India: A review. *Current Science* 73:330-350.

Rao, B. and M.Veerayya. 2000. Influence of marginal highs on the accumulation of organic carbon along the continental slope off western India. *Deep-Sea ResearchPart II* 47:303-327.

Reis, A. T., R. M. C. Maia, C. G. Cilva, M. Rabineau, J. V. Guerra, C. Gorini, A. Ayres, R. Arantes-Oliveira, M. Benabdellouahed, I. Simoes, and R. Tardin.2013. Origin of step-like and lobate seafloor features along the continental shelf off Rio de Janeiro State, Santos basin-Brazil. *Geomorphology* 203:25-45.

Shankar, R. andA. R. Karbassi. 1992.Sedimentological evidence for a palaeobeach off Mangalore, west coast of India.*Journal of the Geological Society of India* 40:241-252.

Shetye, S. R., A. D. Gouveia, S. S. C. Shenoi, D. Sundar, G. S. Michael, A. M. Almeida, andK. Santanam. 1990. Hydrography and circulation off the west coast of India during the southwest monsoon 1987. *Journal of Marine Research* 48:359-378.

Somoza, L., G. Ercilla, V. Urgorri, R. Leon, T. Medialdea, M. Paredes, F. J. Gonzalez, and M. A. Nombela. 2014. Detection and mapping of cold-water coral mounds and living Lophelia reefs in the Galicia Bank, Atlantic NW Iberia margin. *Marine Geology* 349:73-90.

Stanley, H. E., L. A. N. Amaral, A. L. Goldberger, S. Havlin, P. C. Ivanov, and C. K. Peng.1999. Statistical physics and physiology: monofractal and multifractal approaches. *Physica A* 270:309-324.

Stewart, W. K., D. Chu, S. Malik, S. Learner, and H. Singh. 1994. Quantitative seafloor characterization using a bathymetric side scan sonar. *IEEE Journal of Oceanic Engineering* 19:599-610.

Sun, W., G. Xu,P. Gong, and S. Liang. 2006. Fractal analysis of remotely sensed images: A review of methods and applications. *International Journal of Remote Sensing* 27:4963-4990.

Tang, Q., X. Zhou, Z. Liu, and D. Du. 2005.Processing Multibeam Backscatter Data.*Marine Geodesy* 28:251-258.

Telesca, L., V. Lapenna, and F. Vallianatos.2002.Monofractal and multifractal approaches in investigating scaling properties in temporal patterns of the 1983-2000 seismicity in the western Corinth graben, Greece. *Physics of the Earth and Planetary Interiors* 131:63-79.

Thamban, M., V. P. Rao, and S. V. Raju. 1997. Controls on organic carbon distribution in sediments from the eastern Arabian Sea margin. *Geo-Marine Letters* 17:220-227.

Trujillo, A. P. andH. V. Thurman. 2011.*Essentials of Oceanography*, USA: Pearson Education.

Urick, R. J. 1983.*Principles of Underwater Sound*.New York: McGraw-Hill.

Vora, K. H.2007. Past sea level changes along the western continental margin of India: evidence from the morphology of the seabed. Lecture Notes. *Refresher Course in Marine Geology and Geophysics*, National Institute of Oceanography, Dona Paula, India.

Wagle, B. G., K. H. Vora, S. M. Karisiddaiah, M. Veerayya, andF. Almeida. 1994. Holocene submarine terraces on the western continental shelf of India; Implications for sea level changes. *Marine Geology* 117:207-225.

Wen, R.and R. S. Larsen.1996. Mapping oil seeps on the seafloor by Gloria side-scan sonar images a case study from the Northern Gulf of Mexico. *NonrenewableResources* 5:141-154.

Ziegler, M., L. J. Lourens, E. Tuenter, F. Hilgen, G. J. Reichart, and N. Weber. 2010. Precession phasing offset between Indian summer monsoon and Arabian Sea productivity linked to changes in Atlantic overturning circulation. Paleoceanography 25:PA3213.

Figure Caption

Figure1. Multibeam-backscatter imaged map of the study area (part of the western continental margin of India: shown inset) overlain with a bathymetric contour (10 m interval). Five segments (A'-E') are separated based on their backscatter response and rectangles represents their respective sample blocks (A-E). Red and blue arrow shows thedirection of underwater currents during SW monsoon and NE monsoon respectively.

Figure 2. Hybrid slope map of the study area showing seafloor roughness variations. Variations of the local slope are indicated by different colors.

Figure 3. Perspective view of bathymetry depicting seafloor morphology of the central western continental margin of India. Identified geomorphic features and related processes are demonstrated above the bathymetry map.

Figure 4. Single beam (33 kHz) echo-sounder profile across the centre of the study area (15º33′N latitude) showing fault, pockmark, terrace and reef structure. For profile (a) and (b) water depth ranges between 150-200 m and 200-300 m respectively.

Figure 5. SW-NE trending composite sections/profiles corresponding to (a) single channel 4.5 kJ sparker, (b) 3.5 kHz sub-bottom profiler showing the presence of pockmarks, faults, and buried pockmarks. P- pockmarks, F- faults, m- multiple reflectors, Bp- buried pockmark. The scale of x-axes is constant, whereas scale of y-axes is varying.

Figure 6. Distribution of backscattering strength for five blocks (A-E) selected from the broadly segmented areas.

Figure 7. Backscatter image, and bathymetric and backscatter profiles of the blocks (A-E). a) An enlarged view of the backscatter strength of individual blocks (A-E) with pockmarks marked by the blue circles. Inhomogeneous sediment texture variations are also depicted. b) Bathymetric and c) backscatter profiles are drawn based on the data taken from the middle line (N-S direction) of the five blocks (A-E), 1600 m in length. Locations of these blocks are shown in Fig. 1.

Figure 8. Semivariogram of the backscatter strength data of the five blocks (A-E). Estimated ‘D’ values (using the slope of the straight lines) and scale breaks are given in Table 2.

Figure 9. Backscatter strength (dB) normalized PDFs and fitted curves for total and component PDFs.

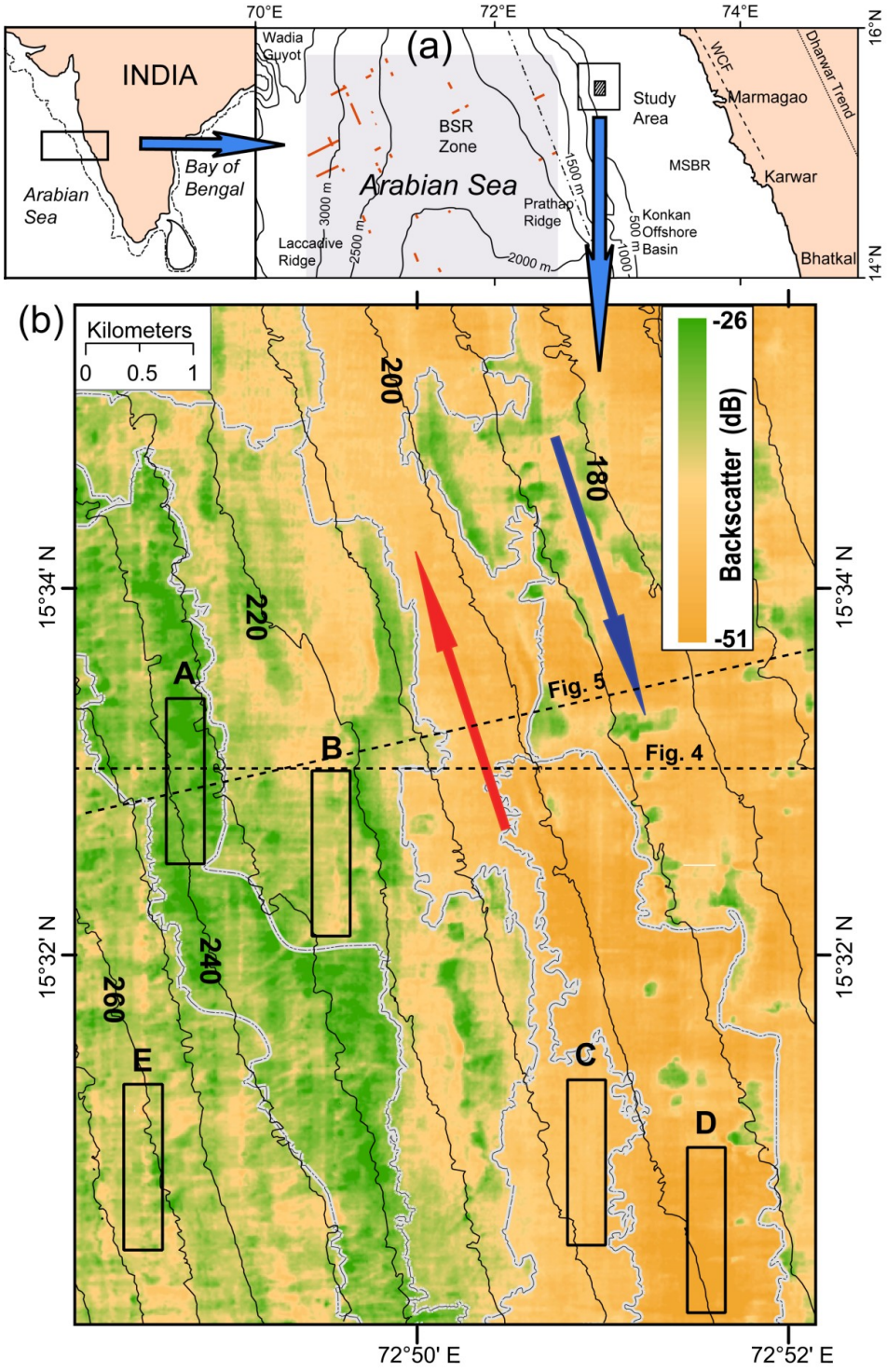

Figure 1. Multibeam-backscatter imaged map of the study area (part of the western continental margin of India: shown inset) overlain with a bathymetric contour (10 m interval). Five segments (A'-E') are separated based on their backscatter response and rectangles represents their respective sample blocks (A-E). Red and blue arrow shows thedirection of underwater currents during SW monsoon and NE monsoon respectively.

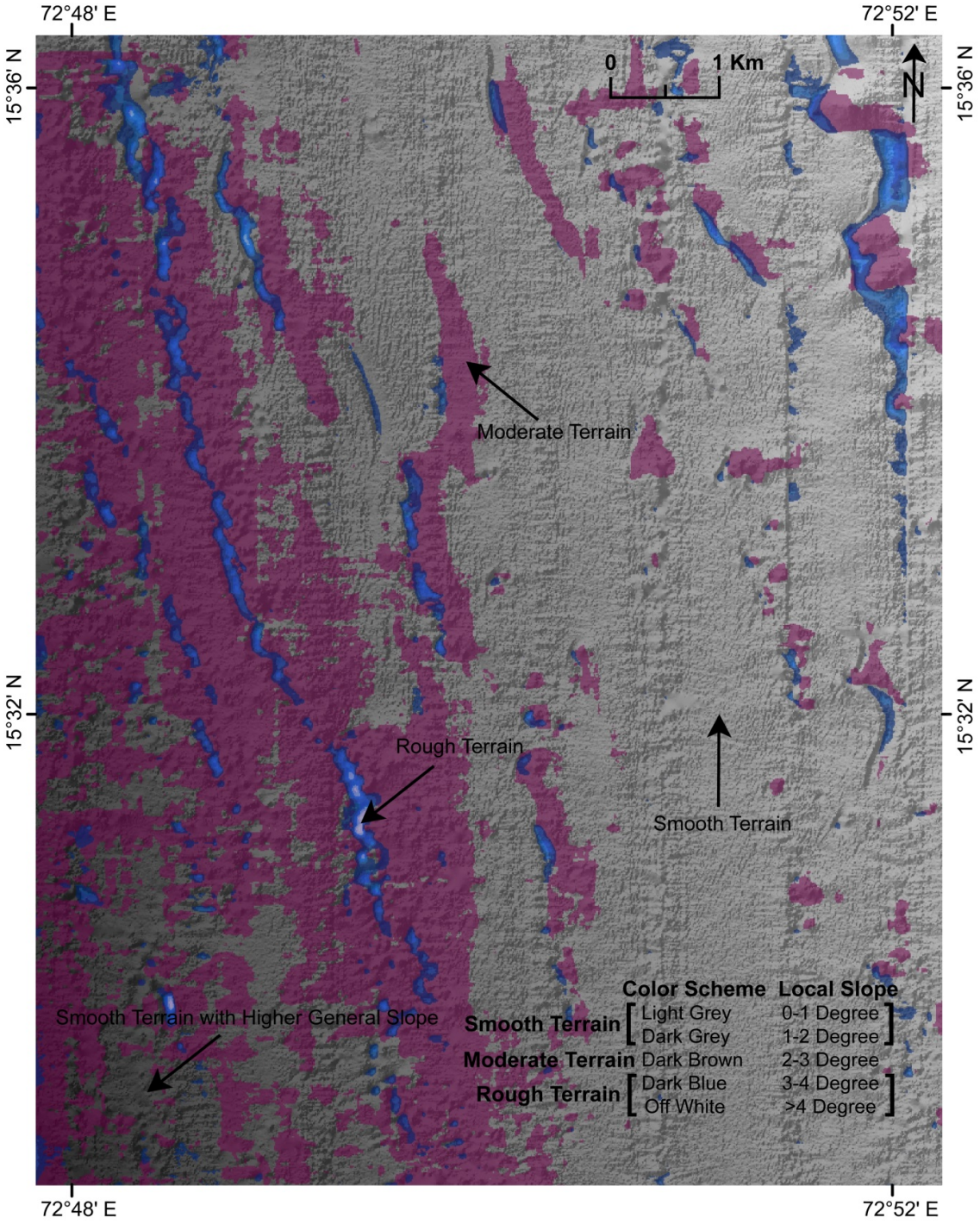

Figure 2. Hybrid slope map of the study area showing seafloor roughness variations. Variations of the local slope are indicated by different colors.

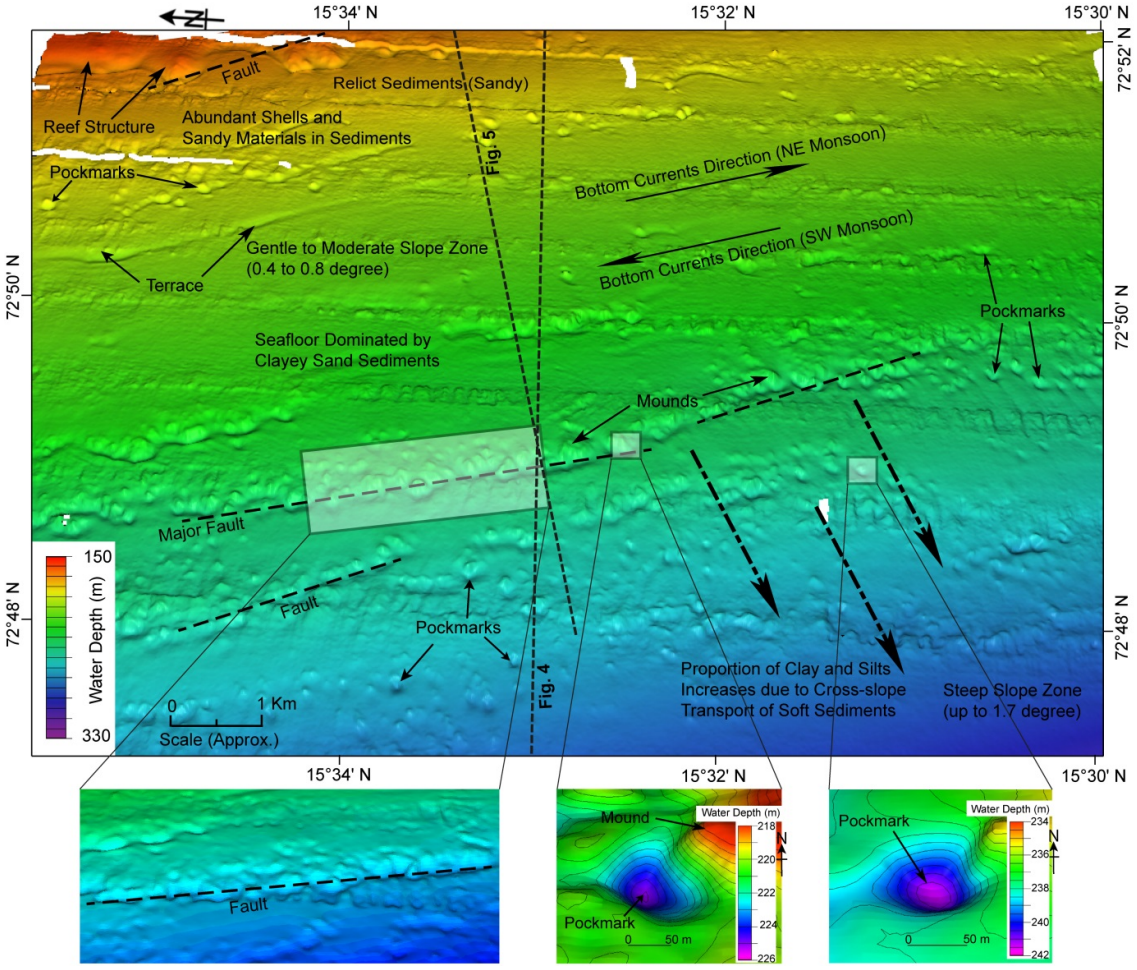

Figure 3. Perspective view of bathymetry depicting seafloor morphology of the central western continental margin of India. Identified geomorphic features and related processes are demonstrated above the bathymetry map.

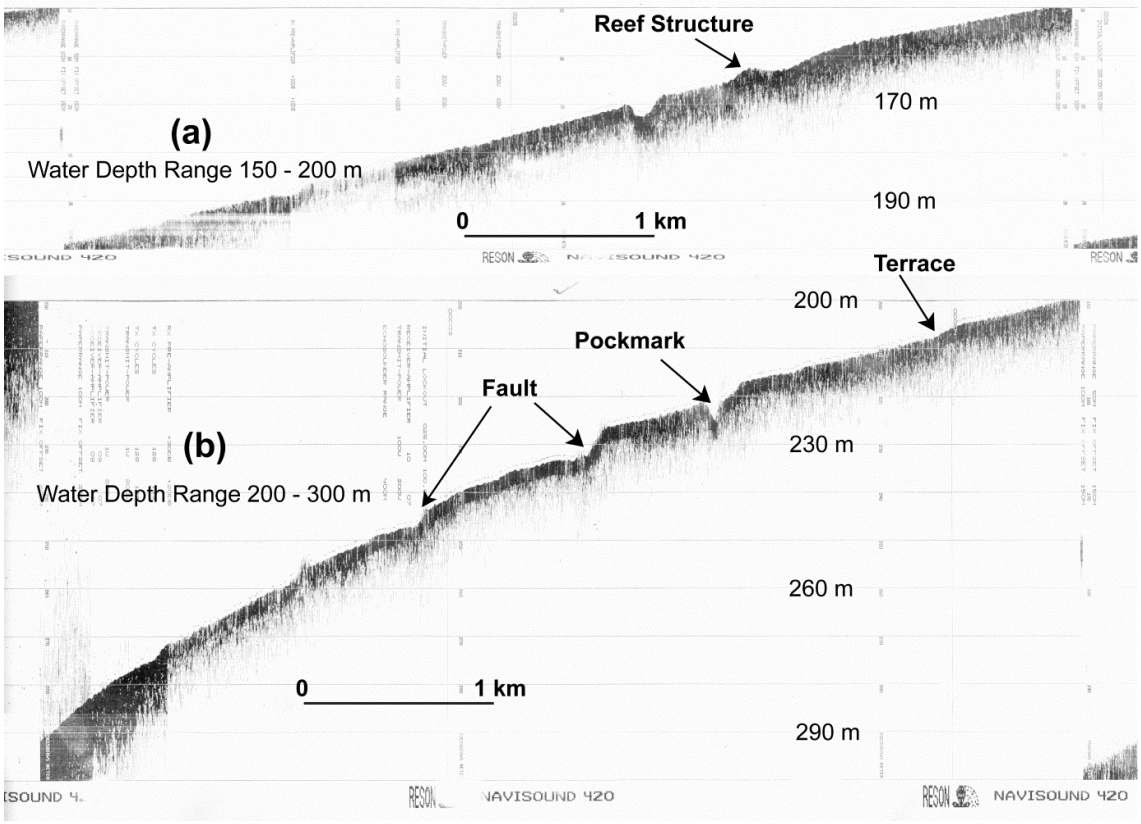

Figure 4. Single beam (33 kHz) echo-sounder profile across the centre of the study area (15º33′ N latitude) showing fault, pockmark, terrace and reef structure. For profile (a) and (b) water depth ranges between 150-200 m and 200-300 m respectively.

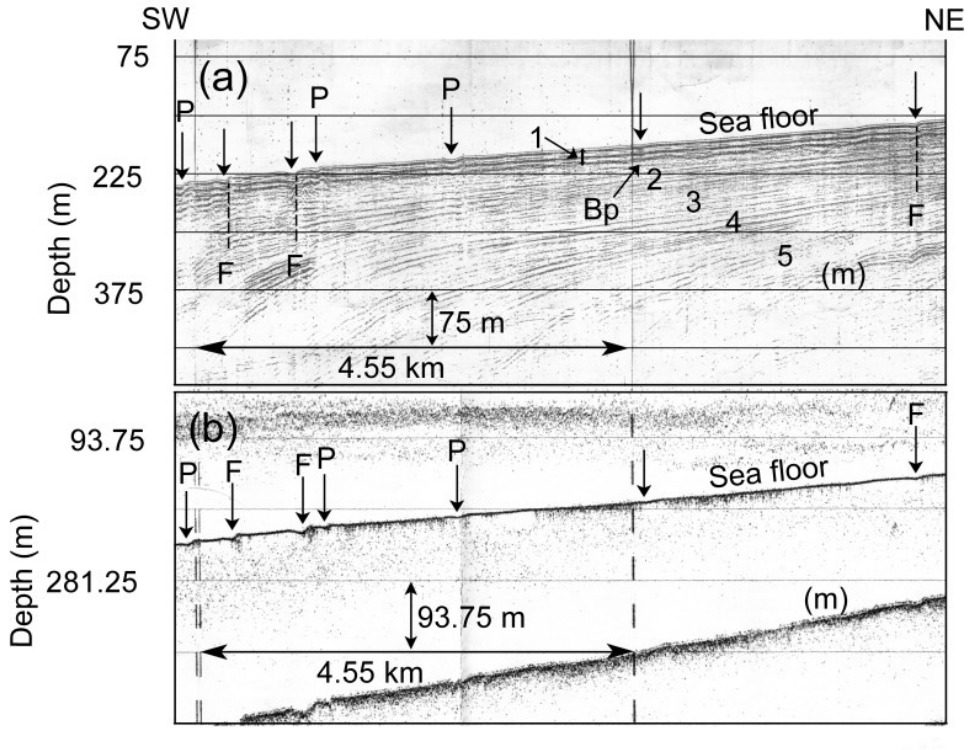

Figure 5. SW-NE trending composite sections/profiles corresponding to (a) single channel 4.5 kJ sparker, (b) 3.5 kHz sub-bottom profiler showing the presence of pockmarks, faults, and buried pockmarks. P- pockmarks, F- faults, m- multiple reflectors, Bp- buried pockmark. The scale of x-axes is constant, whereas scale of y-axes is varying.

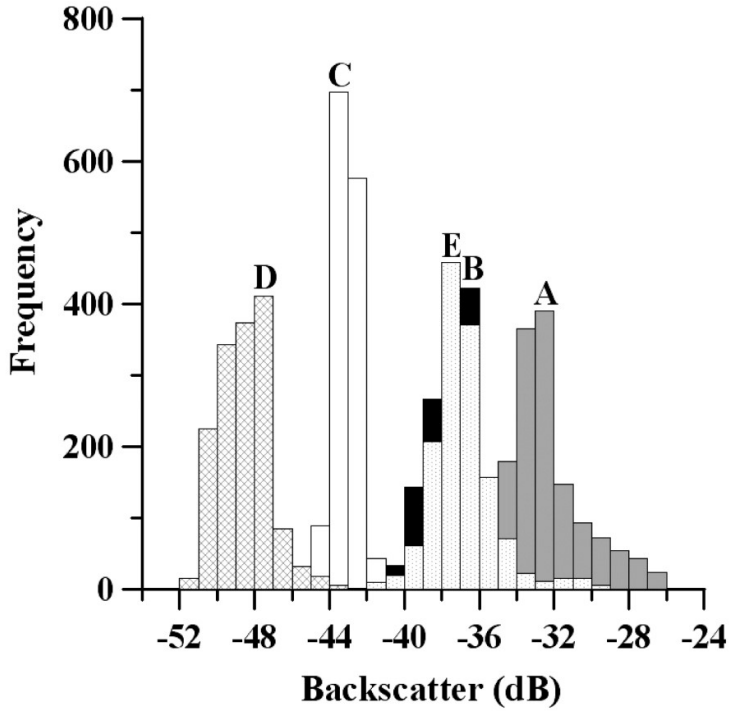

Figure 6. Distribution of backscattering strength for five blocks (A-E) selected from the broadly segmented areas.

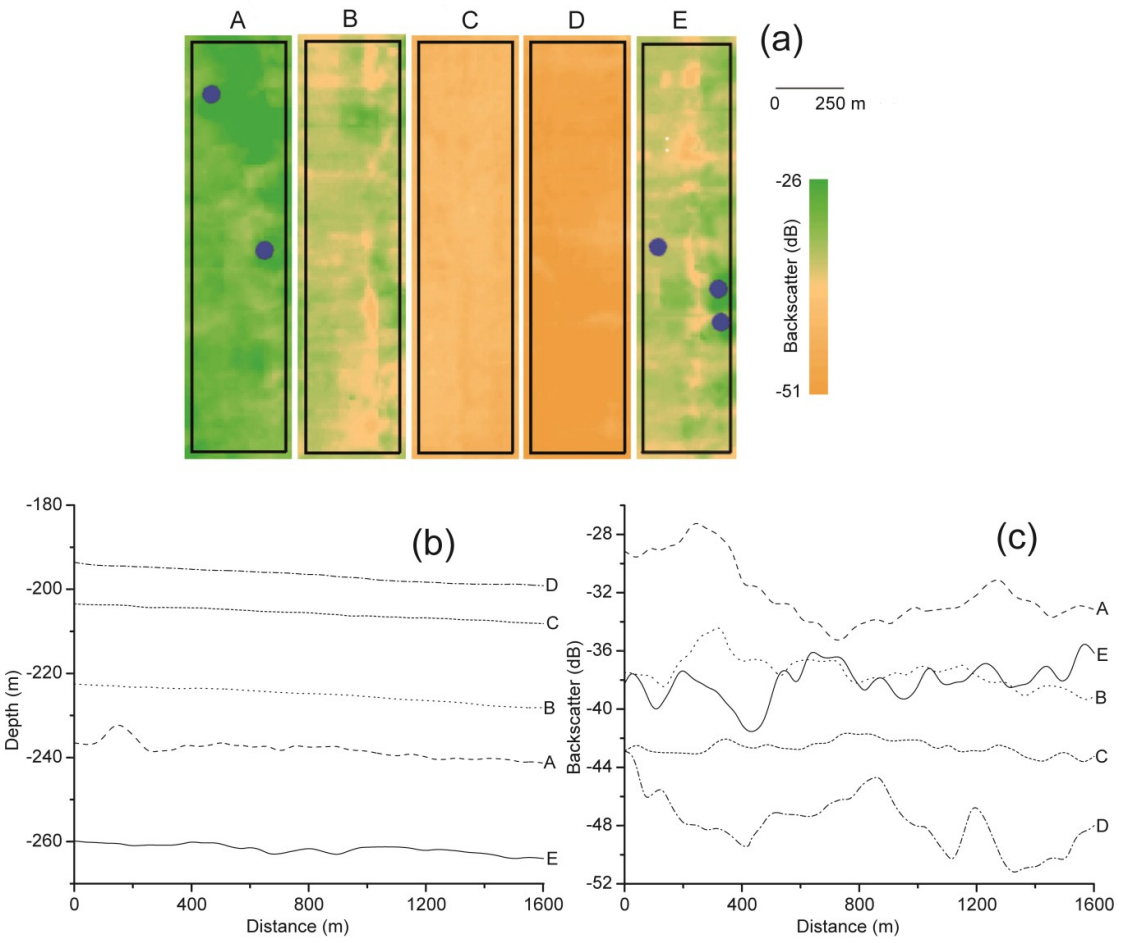

Figure 7. Backscatter image, and bathymetric and backscatter profiles of the blocks (A-E). a) An enlarged view of the backscatter strength of individual blocks (A-E) with pockmarks marked by the blue circles. Inhomogeneous sediment texture variations are also depicted. b) Bathymetric and c) backscatter profiles are drawn based on the data taken from the middle line (N-S direction) of the five blocks (A-E), 1600 m in length. Locations of these blocks are shown in Fig. 1.

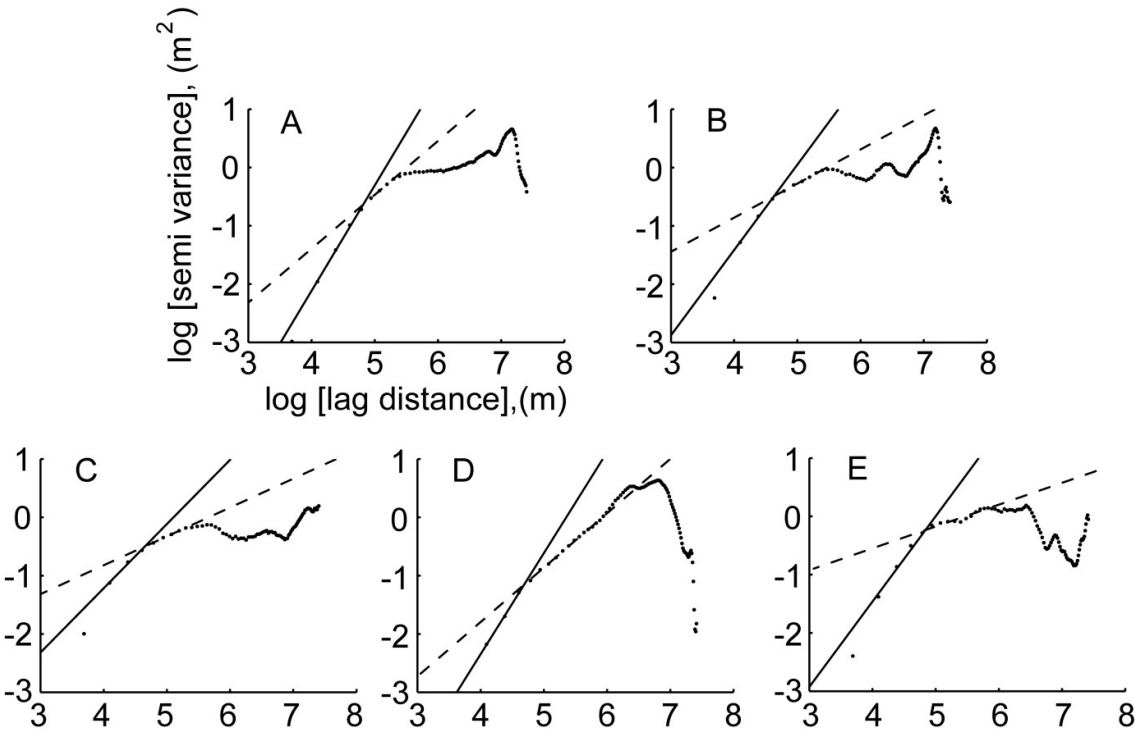

Figure 8. Semivariogram of the backscatter strength data of the five blocks (A-E). Estimated 'D' values (using the slope of the straight lines) and scale breaks are given in Table 2.

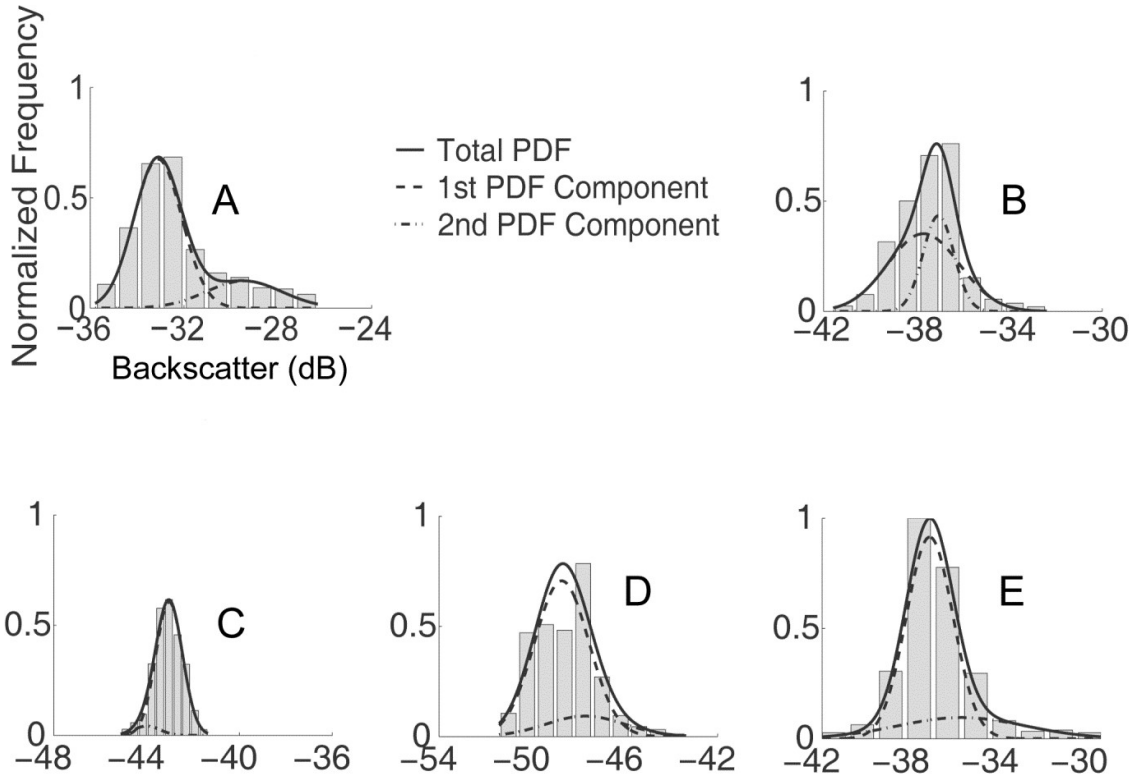

Figure 9. Backscatter strength (dB) normalized PDFs and fitted curves for total and component PDFs.

Table 1: Backscatter data details of the segments and blocks

		Total data points	Min. backscatter (dB)	Max. backscatter (dB)	Mean backscatter (dB)	Backscatter range assigned for segmentation (dB)	Percentage of data points falling between the ranges
Segments	A'	21882	-37.0	-26.0	-32.7	-35 to -30	88.0
	B'	31277	-42.0	-30.5	-37.6	-40 to -35	91.8
	C'	33699	-45.7	-37.0	-42.5	-45 to -40	97.1
	D'	17324	-51.4	-32.8	-47.0	-50 to -45	90.1
	E'	35422	-42.8	-29.4	-36.8	-40 to -30	95.4
Blocks	A	1411	-35.8	-26.3	-32.3	-35 to -30	85.5
	B	1428	-41.6	-32.4	-37.4	-40 to -35	93.3
	C	1411	-45.1	-41.4	-43.1	-45 to -40	99.8
	D	1512	-51.4	-43.4	-48.5	-50 to -45	82.5
	E	1428	-42.1	-29.4	-36.9	-40 to -30	97.3

Table 2: Estimated fractal dimensions and scale breaks of the study blocks

Blocks	Slope	Intercept	Fractal dimension ('D')	Scale break distance (in metre)	Correlation Coefficient (R^2)
A	1.80	-9.4	2.10	60-120	0.99
	0.92	-5.1	2.54	140-200	0.99
B	1.50	-7.3	2.25	60-100	0.99
	0.59	-3.2	2.71	120-220	0.99
C	1.10	-5.6	2.45	60-100	0.99
	0.50	-2.8	2.75	120-200	0.99
D	1.70	-9.3	2.15	60-100	0.99
	0.93	-5.5	2.54	120-380	0.99
E	1.50	-7.3	2.25	60-140	0.99
	0.37	-2.1	2.82	160-360	0.95

Table 3: PDF parameters of backscatter strength data of different study blocks

Blocks	Mean PDF position for total curve (dB)	Mean PDF for 1st comp. (dB)	Mean PDF for 2nd comp. (dB)	Std. Dev. for total PDF curve	Std. Dev. for 1st comp.	Std. Dev. for 2nd comp.	Proportion of the 1st comp. (%)	Proportion of the 2nd comp. (%)
A	-32.3	-33.1	-29.4	1.93	1.02	1.61	78	22
B	-37.4	-37.1	-37.7	1.34	0.67	1.55	35	65
C	-43.1	-43.0	-44.0	0.63	0.58	0.57	94	06
D	-48.5	-48.7	-47.7	1.34	1.17	1.69	84	16
E	-36.9	-37.2	-35.8	1.72	1.05	2.86	78	22